Supporting information for

A transition path ensemble study reveals a linchpin role for Mg^{2+} during rate-limiting ADP release from protein kinase A

Ilja V. Khavrutskii,[a,b,c*] Barry Grant,[b,c] Susan S. Taylor,[a,c,d] and J. Andrew McCammon[a,b,c,d]

Running Title: A linchpin role for Mg^{2+} in ADP release from PKA

[a)]Howard Hughes Medical Institute

[b)]Center for Theoretical Biological Physics

[c)]Department of Chemistry and Biochemistry

[d)]Department of Pharmacology

University of California San Diego, La Jolla, California 92093-0365

[*]Corresponding Author E-mail: ikhavru@mccammon.ucsd.edu
University of California, San Diego
Urey Hall, Room 4206
9500 Gilman Dr. M/C 0365
La Jolla, CA 92093-0365
Tel: (858) 366-3090
Fax: (858) 534-4974

Funding: This work was in part supported by grants from NIH, NSF, NBCR, CTBP and HHMI, including NIH grant GM19301.

Full reference 63 from the main text:

(63) MacKerell Jr., A. D.; Bashford, D.; Bellott, M.; Dunbrack Jr., R. L.; Evanseck, J. D.; Field, M. J.; Fischer, S.; Gao, J.; Guo, H.; Ha, S.; Joseph-McCarthy, D.; Kuchnir, L.; Kuczera, K.; Lau, F. T. K.; Mattos, C.; Michnick, S.; Ngo, T.; Nguyen, D. T.; Prodhom, B.; Reiher III, W. E.; Roux, B.; Schlenkrich, M.; Smith, J. C.; Stote, R.; Straub, J.; Watanabe, M.; Wiorkiewicz-Kuczera, J.; Yin, D.; Karplus, M. *J. Phys. Chem. B* **1998**, *102*, 3586-3616.

Figure 1S A

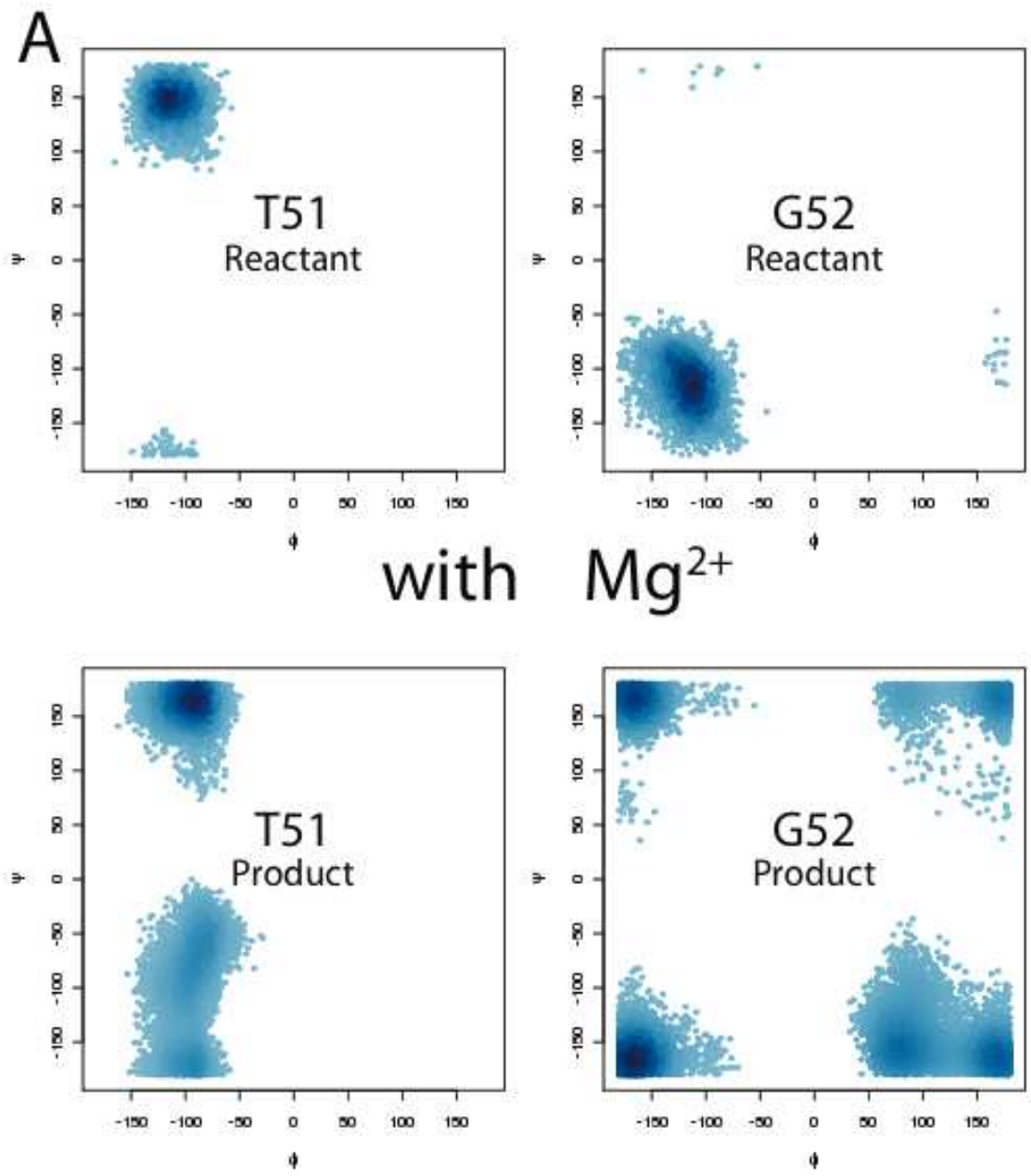
A
T51
Reactant
G52
Reactant
with Mg2+
T51
Product
G52
Product
ψ
ϕ
-150 -100 -50 0 50 100 150

Figure 1S B

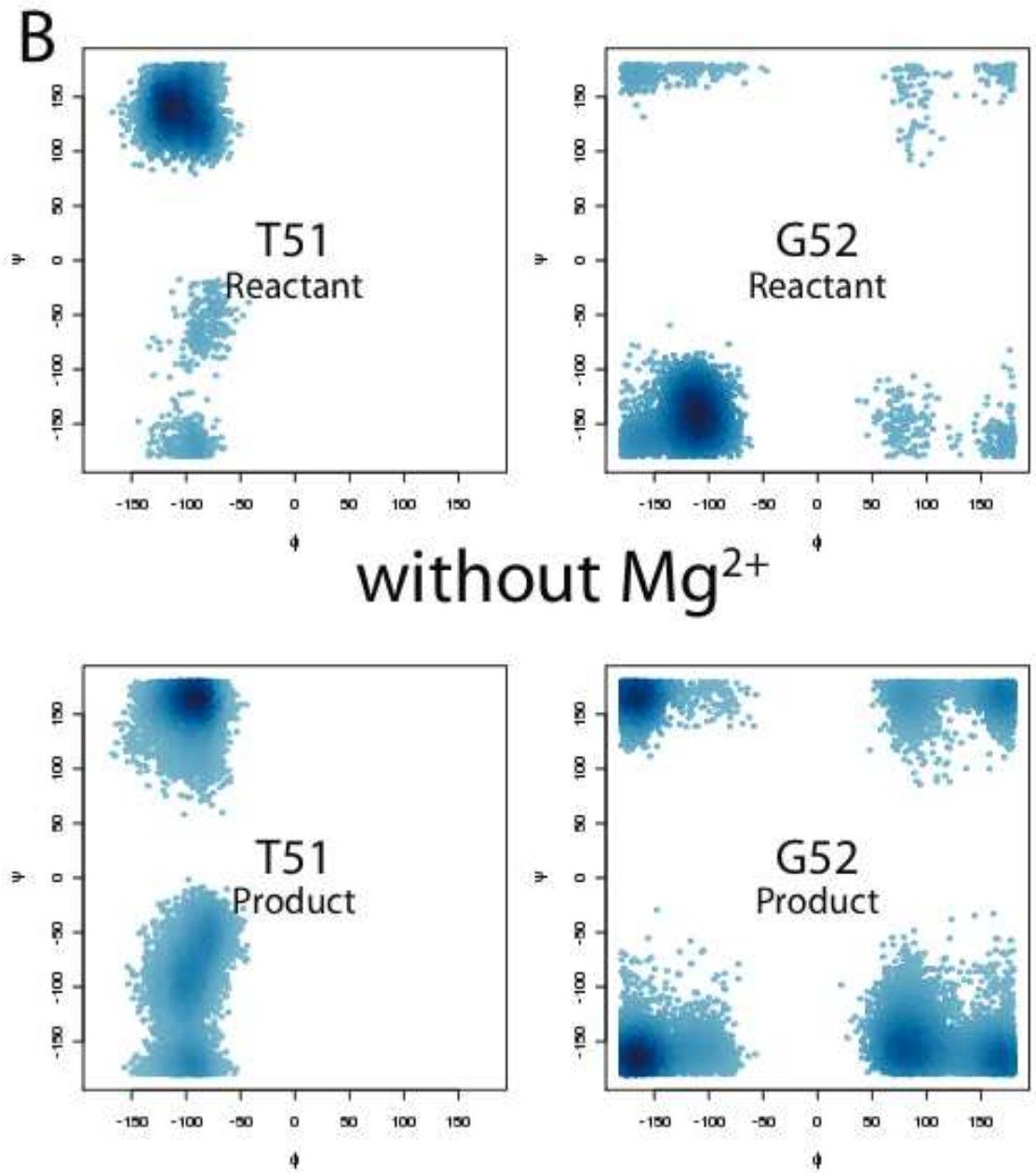

Ramachandran plot for the main backbone dihedral angles ϕ and ψ of residues T51 and G52 from the Gly-rich loop. Section **A:** with two Mg^{2+} ions bound to ADP, and section **B:** with no Mg^{2+} ions bound. Top and bottom of each section correspond to reactant and product states respectively. The reactant state is a collection of beads 1 through 18 and has ADP in the binding pocket of PKA. The product state encompasses beads 113

through 185 and the ADP molecule placed at distances where no interactions could be detected. Dihedral analysis and figure were made using Bio3D program.

Methods

The system setup proceeded from the X-ray crystallographic structure of transition state analogue of 1L3R by removing AlF_3 and the phosphorylated substrate peptide. This leaves the catalytic subunit complexed with two Mg^{2+} ions and an ADP molecule. The PDB structure was missing nine N-terminal residues 5 through 13, which were modeled in by building a straight polypeptide chain leaving a sizable separation between the atoms of the peptide bond between residues 13 and 14. Starting from this extended fragment its coordinates were optimized to a normal peptide bond length as follows. Initially, all the atoms of the protein except those of missing residues were fixed, and the backbone of the missing residues was restrained harmonically initially with a force constant of 100 kcal/(mol*$Å^2$) further mass-weighted. Using steepest descent optimization for 1000 steps the restraint was progressively released to 50, 25, 10, 5, 1 and 0.01. At the last restraint the optimization has been repeated for three more times. Finally, four more runs were performed without force constant using two SD and two ABNR runs. This was done in the gas phase for computational convenience. Although most of the residues behaved well under the optimization conditions, the peptide bond between residues 13 and 14 was established in the cis conformation. Regardless, the modeled piece remained highly flexible throughout the simulations, mimicking the experimentally observed disorder. Furthermore, the modeled loop was sufficiently remote from the active site not to affect the results significantly. We have subsequently turned the cis conformation to trans to verify that it had no significant effect on the dynamics of the remaining, well-resolved part of the enzyme.

We protonated histidines 62, 68, 87, 142, 158 and 260 to have a positive charge, while histidines 131 and 294 were left neutral with the proton on Nε. The assignment of histidine protonation state was done through inspection of their nearest neighbor environment. In addition, residues S10, S139, T197, S338 were phosphorylated, each group contributing -2 charge. Note that phosphorylated residue S10 was in the disordered region.

To have a solid reference system during the path optimization we picked a set of residues from four relatively rigid helices in the large, C-terminal lobe. Specifically, we fixed Cα atoms of residues 140:160, 217:234, 263:274, 288:298 of helices 6, 10, 12, 13-14.

To neutralize the system we employed total of 31 Cl^-, 23 Na^+, 4 Mg^{2+}. The rectangular simulation box 79 x 88 x 69 Å was filled with 13,103 water molecules.

To generate the product state the ADP was translated outside the active site along a direction that visually presented little steric clashes to one of the corners of the simulation box. Note that Mg^{2+} ions bound at the active site were not translated along with the ADP. For the path activation we used initially 24 beads. Activated evolution procedure was followed to span the path between the reactant and the product. We used relatively soft force constant 0.05 kcal/mol/$Å^2$ on all the heavy atoms of the solute except those fixed. The reactive coordinate space for the activated evolution procedure comprised all of the heavy atoms of the protein except the fixed portion of the four helices of the rigid core. Activation started from the reactant state that corresponded to the 1L3R structure with the ADP bound and every 60 ps evolution step a new bead was activated. This procedure was continued for 24 steps until all the 24 beads were activated. Every time a new path was generated, the new reference beads were realigned using the rigid portion of the large lobe as a reference frame. Thus the fixed portion maintained its precise coordinates in all the beads. We would like to note that we did restraint the Mg^{2+} ions. However, at the beginning of the activation procedure, our product state had Mg^{2+} ions bound to their original positions in the crystal structure. After running activated evolution for 20 steps in all of which Mg^{2+} ions followed closely the ADP, we changed the product state by translating the Mg^{2+} ions as well. This prevented collapse of the Mg^{2+} ions back to the bound state. With that we completed the activation step after four more steps such that in the end the product state Mg_2ADP was in the same conformation as it was in the bound state.

After the path was activated we continued optimization with all the beads now activated including the reactant and product endpoints. During optimization we employed the

following RCSs. Note that at step 391 we changed the RCS from all heavy atoms to the backbone atoms only and further excluded certain atoms of the ADP molecule.

The following RCSs are defined using the CHARMM scripting language and the CHARMM27 forcefield.

RCS1

```
define fbuf sele (segi prot .and. (resi 140:160 .or. resi 217:234 .or. resi 263:274 .or. resi 288:298)) .and. type ca end
define rcs sele .not. hydrogen .and. .not. fbuf end
```

In addition to the protein and ADP, RCS1 also included two Mg^{2+} ions that were bound to ADP. No water molecule or other ions were included by construction.

RCS2

At step 391 the RCS1 has changed to the following RCS2:

```
define sadp sele segi adpr .and. -
(type c4' -
.or. type o4' -
.or. type c1' -
.or. type c5 -
.or. type n7 -
.or. type c8 -
.or. type n9 -
.or. type n1 -
.or. type c2 -
.or. type n3 -
.or. type c4 -
.or. type c6 -
.or. type n6 -
.or. type c5' -
.or. type o5' -
.or. type pa -
.or. type o1a -
.or. type o2a -
.or. type o3a -
.or. type pb -
.or. type o1b -
.or. type o2b -
.or. type o3b) -
end

!define lowest backbone level
```

```
define level1 sele type c -
 .or. type n -
 .or. type ca -
 .or. type nt -
 .or. type cy -
 .or. type cay -
 .or. type cat end

!this defines space fbuf that needs to be fixed
define fbuf sele (segi prot .and. (resi 140:160 .or. resi 217:234 .or. resi
288:298)) -
 .and. type ca -
 end

define rcs sele ((segi prot .and. level1) -
 .or. sadp .or. segi ions) -
 .and. .not. fbuf -
 end
```

Finally to compute PMFs, RCS2 was further reduced to RCS3:

RCS3

```
define sadp sele segi adpr .and. -
(type c4' -
.or. type o4' -
.or. type c1' -
.or. type c5 -
.or. type n7 -
.or. type c8 -
.or. type n9 -
.or. type n1 -
.or. type c2 -
.or. type n3 -
.or. type c4 -
.or. type c6 -
.or. type n6 -
.or. type c5' -
.or. type o5' -
.or. type pa -
.or. type o1a -
.or. type o2a -
.or. type o3a -
.or. type pb -
.or. type o1b -
.or. type o2b -
```

```
.or. type o3b) -
end

!define lowest backbone level
define level1 sele type c -
 .or. type n -
 .or. type ca -
 .or. type nt -
 .or. type cy -
 .or. type cay -
 .or. type cat end

!this defines space fbuf that needs to be fixed
define fbuf sele (segi prot .and. (resi 140:160 .or. resi 217:234 .or. resi 263:274 .or. resi
288:298)) -
 .and. type ca -
 end

!we don't really need to worry about fbuf at this stage, so we do this for clarity
define rcs sele sadp .or. segi ions -
 .or. fbuf -
 end
```

Optimization protocol. No enhancement of the HFB steepest descent step was performed, corresponding to the step size of 0.0.

Steps	Beads	Trunc	Force constant	RCS
24-40	24	22	0.05	1
41-170		18	0.05	1
171-241		18	0.1	1
242-260		18	0.25	1
261-301	47	32	0.25	1
302-310		32	0.5	1
311-330		36		
331-340	93	62	0.5	1
341		82	0.5	1
342-			1.0	1
343-361			2.0	1
362-373			5.0	1
374-392		90	5.0	1
393-410		82	5.0	2
411-430	185	164	5.0	2
431-451		172	5.0	2

In summary, following activation, we employed 24 beads for 260 steps before inserting additional beads between the existing ones to make a total of 47 beads. Steps 261-330 used 47 beads; steps 331-340 - 93 beads; steps 341-410 - 93 beads with an updated protocol for generating references within charmm script. Finally steps 411 to 450 were run using 185 beads.

For the free energy decomposition we defined contributions from the ADP as follows:

Nucleotide

```
!define part of the ADP that is not fidgeting
define sadp sele segi adpr .and. -
(type c5 -
.or. type n7 -
.or. type c8 -
.or. type n9 -
.or. type n1 -
.or. type c2 -
.or. type n3 -
.or. type c4 -
.or. type c6 -
.or. type n6) -
end

define rcs sele sadp -
  end
```

Ribose

```
!define part of the ADP that is not fidgeting
define sadp sele segi adpr .and. -
(type c4' -
.or. type o4' -
.or. type c1' -
.or. type c5' -
.or. type o5') -
end

define rcs sele sadp -
  end
```

Pyrophosphate

```
!define part of the ADP that is not fidgeting
define sadp sele segi adpr .and. -
(type pa -
.or. type o1a -
```

```
.or. type o2a -
.or. type o3a -
.or. type pb -
.or. type o1b -
.or. type o2b -
.or. type o3b) -
end

define rcs sele sadp -
  end
```

These degrees of freedom were integrated using the standard HFB line integral approach for calculating work.

Finally the protein contribution was determined from the rigid helices positions only, all the other degrees of freedom were assumed to have averaged out.

Protein

```
!define lowest backbone level
define level1 sele type c -
 .or. type n -
 .or. type ca -
 .or. type nt -
 .or. type cy -
 .or. type cay -
 .or. type cat end

!this defines space fbuf that needs to be fixed
define fbuf sele (segi prot .and. (resi 140:160 .or. resi 217:234 .or. resi 263:274 .or. resi
288:298)) -
 .and. type ca -
 end

!we don't really need to worry about fbuf at this stage, so we do this for clarity
define rcs sele fbuf -
 end
```

Next section details comparative Bio3D analysis of the PKA structures that are present in the PDB and have been generated by the simulations of the present work.

Expanded Results and Discussion

Transport of ions by carboxylate shifts

Analysis of the RCS2 optimized transition path ensemble (see Methods) in the direction from apo, product to ADP-bound, reactant state indicates that during the relay Mg1 and Mg2 ions contact the carboxylic group of E170 at about the same time (Figure 2S). Initially, Mg1 coordinates E170 in a monodentate fashion, but soon shifts to a bidentate coordination mode with the help of a carbonyl oxygen from T51 of the Gly-rich loop. When Mg1 shifts from a bidentate to monodentate coordination it moves further into the active site and leads to the bidentate coordination of Mg2 by E170. Mg1 then tethers N171, while still coordinated by the carbonyl of T51. Mg2 remains bidentate with respect to E170 whilst Mg1 coordinates D184 in a monodentate fashion along with N171. Mg2 then shifts further to coordinate N171 and E170 in a monodentate fashion. Eventually, D184 shifts to coordinate Mg1 in a bidentate mode, whereas Mg2 moves between E170 and D184 complemented by N171. Finally, E170 breaks away from Mg2 leaving both ions in their familiar bound states.

[Figure 2S here]

Three cation-binding sites created by nucleotide binding

Little is known about the process of Mg^{2+} association with PKA. Before the structure of PKA became available, the activating Mg^{2+} ion was thought to reside exclusively on the phosphates of ATP, with the inhibitory ion protein bound. In the absence of nucleotide, ions were found to bind nonspecifically to PKA, suggesting the lack of a well defined binding site on the enzyme.(*1-4*) Studies with Co^{3+}ATP, that is inert with respect to metal

exchange, suggested that the nucleotide binding site was occupied by ATP with an associated Co^{3+} ion.(*1, 2*) It is known experimentally that the chelating coordination of Co^{3+} and Mg^{2+} by adjacent phosphates, one of which is terminal, provides tight coordination for an ion in solution.(*1, 2, 5*) Moreover, the bulk of cellular Mg^{2+} is bound with ATP.(*6*) Therefore, by analogy with Co^{3+}, one Mg^{2+} ion can be brought into the active site with ATP. The other likely comes from solution, once the nucleotide is bound. Alternatively, both ions can come from solution once ADP is bound. Crystal soaking at higher Mg^{2+} concentrations is consistent with either proposal.(*7*)

Our simulations demonstrate that in the absence of ADP, the active site of PKA coordinates no cations. Therefore we conjecture that adenine-driven nucleotide binding to PKA creates the specific cation-binding sites at the PKA/ADP interface. Specifically, once adenine anchors in its highly conserved binding site, the two covalently linked groups, namely ribose and pyrophosphate create a total of three cation-binding sites.

Two of these sites employ the pyrophosphate group in cooperation with the protein to coordinate the Mg^{2+} ions acting as linchpins. However, our simulations indicate that Mg^{2+} ions are more strongly bound to the pyrophosphate group than to the protein. Indeed, Mg^{2+} ions follow ADP outside the active site even when weakly biased to stay in the active site.

The third, high affinity cation binding site emerges from the ribose hydroxyl groups and neighboring enzyme residues (E127, Y330). None of these groups in isolation is strong

enough to provide high affinity binding to cations by itself. It is currently unknown if this third binding site is important for ADP binding. However, we note the coordination of an absolutely conserved Arg residue in the P-3 position of substrate and inhibitor peptides at this site.(*7*) Accordingly, removal of the 2'-OH group that contributes to the high affinity cation binding site has been shown to increases the binding constant for the RI inhibitor. Importantly, MgATP binding to catalytic subunit itself is quite poor (K_d is on the order of 10 μM), whereas the presence of a substrate or an inhibitor dramatically enhances binding (K_d decreases to 10-20 nM).

Thus the third site may operate as a functionally important sensor for the closed C-subunit with bound nucleotide. This conditional binding site may be responsible for the absolute requirement of Mg^{2+}-nucleotide binding to PKA to form complexes with RI inhibitor or PKI,(*8-12*) and determining the specific order of the underlying binding events.(*4, 9, 12-14*)

DFG Flip

The DFG conformational change would flip D184 from its unfavorable αL backbone configuration into more favorable pII-like backbone configuration.(*15-18*) At the same time the favorable polar environment of D184 will switch to unfavorable hydrophobic environment. Therefore the DFG flip toggles the system between active and inactive states. It is worth noting that although rare for non-Gly side chains, energetically unfavorable αL backbone configurations are common to binding sites of different proteins.(*19*) Embedding the D184 side chain in the hydrophobic environment of the

inactive state by means of DFG flip has been inferred to cause its protonation in Abl kinase.(*16, 20*) In PKA, the DFG-flip has not been demonstrated. However, recent NMR studies indicate a possibility of DFG-flip in PKA in solution.(*13*)

Because all available crystal structures of PKA, including apoenzyme, have the DFG motif in the active conformation, it is likely that during PKA catalysis the enzyme will maintain its active conformation. Our simulations support this notion. Specifically, the DFG motif remains in the active conformation along the whole path of ADP release from the binary complex to the apoenzyme. In agreement, previous MD simulations on Abl kinase have suggested that the DFG flip is a rare event.(*20*) Our study suggests further that the DFG flip is off path for the nucleotide release.

We believe that the DFG flip in the closed state with ADP and Mg^{2+} ions bound would be strongly unfavorable due to the Mg^{2+} coordination of the DFG motif through the D184 residue. Therefore, similar to ADP release, the DFG flip would require prior Mg^{2+} dissociation.

Figure 2S

Mg^{2+} binding relay featuring carboxylate shifts with residues E170 and D184. The Mg^{2+} ions remain associated with ADP throughout the binding. Six representative stages, **a** through **f** are shown.

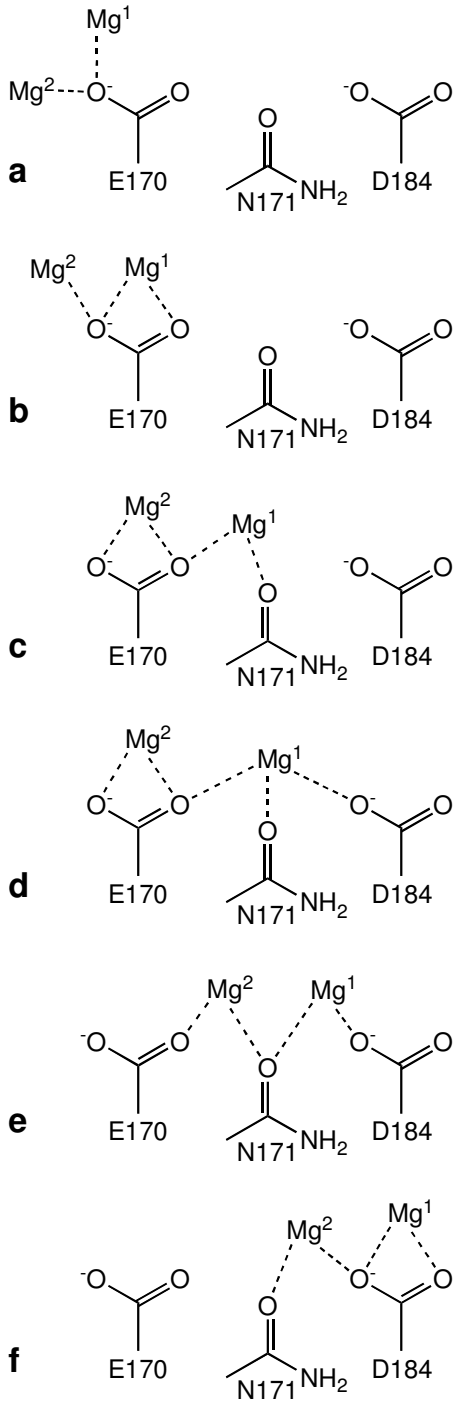

References

1. Armstrong, R. N., Kondo, H., Granot, J., Kaiser, E. T., and Mildvan, A. S. (1979) Magnetic Resonance and Kinetic Studies of the Manganese(II) Ion and Substrate Complexes of the Catalytic Subunit of Adenosine 3',5'-Monophosphate Dependent Protein Kinase from Bovine Heart, *Biochemistry 18*, 1230-1238.
2. Granot, J., Mildvan, A. S., and Kaiser, E. T. (1980) Studies of the Mechanism of Action and Regulation of cAMP-Dependent Protein Kinase, *Arch. Biochem. Biophys. 205*, 1-17.
3. Cook, P. F., Neville Jr., M. E., Vrana, K. E., Hartl, T. F., and Roskoski Jr., R. (1982) Adenosine Cyclic 3',5'-Monophosphate Dependent Protein Kinase: Kinetic Mechanism for the Bovine Skeletal Muscle Catalytic Subunit, *Biochemistry 21*, 5794-5799.
4. Qamar, R., Yoon, M.-Y., and Cook, P. F. (1992) Kinetic Mechanism of the Adenosine 3',5'-Monophosphate Dependent Protein Kinase Catalytic Subunit in the Direction of Magnesium Adenosine 5'-Diphosphate Phosphorylation, *Biochemistry 31*, 9986-9992.
5. Huang, S. L., and Tsai, M. D. (1982) Does the magnesium(II) ion interact with the alpha-phosphate of ATP? An investigation by oxygen-17 nuclear magnetic resonance, *Biochemistry 21*, 951-959.
6. Gabriel, T. E., and G¸nzel, D. (2007) Quantification of Mg2+ extrusion and cytosolic Mg2+-buffering in Xenopus oocytes, *Arch. Biochem. Biophys. 458*, 3-15.
7. Zheng, J., Knighton, D. R., Ten Eyck, L. F., Karlsson, R., Xuong, N. H., Taylor, S. S., and Sowadski, J. M. (1993) Crystal Structure of the Catalytic Subunit of cAMP-Dependent Protein Kinase Complexed with MgATP and Peptide Inhibitor, *Biochemistry 32*, 2154-2161.
8. Corbin, J. D., Keely, S. L., and Park, C. R. (1975) The distribution and dissociation of cyclic adenosine 3':5'-monophosphate-dependent protein kinases in adipose, cardiac, and other tissues, *J. Biol. Chem. 250*, 218-225.
9. Whitehouse, S., and Walsh, D. A. (1983) Mg X ATP2-dependent interaction of the inhibitor protein of the cAMP- dependent protein kinase with the catalytic subunit, *J. Biol. Chem. 258*, 3682-3692.
10. Van Patten, S. M., Fletcher, W. H., and Walsh, D. A. (1986) The inhibitor protein of the cAMP-dependent protein kinase-catalytic subunit interaction. Parameters of complex formation, *J. Biol. Chem. 261*, 5514-5523.
11. Neitzel, J. J., Dostmann, W. R. G., and Taylor, S. S. (1991) Role of magnesium-ATP in the activation and reassociation of cAMP-dependent protein kinase I: consequences of replacing the essential arginine in cAMP-binding site A, *Biochemistry 30*, 733-739.
12. Herberg, F. W., and Taylor, S. S. (1993) Physiological inhibitors of the catalytic subunit of cAMP-dependent protein kinase: effect of MgATP on protein-protein interactions, *Biochemistry 32*, 14015-14022.
13. Masterson, L. R., Mascioni, A., Traaseth, N. J., Taylor, S. S., and Veglia, G. (2008) Allosteric cooperativity in protein kinase A, *Proc. Nat. Acad. Sci. USA 105*, 506-511.

14. Zimmermann, B., Schweinsberg, S., Drewianka, S., and Herberg, F. W. (2008) Effect of metal ions on high-affinity binding of pseudosubstrate inhibitors to PKA, *Biochem. J. 413*, 93-101.
15. Kornev, A. P., Haste, N. M., Taylor, S. S., and Eyck, L. F. (2006) Surface comparison of active and inactive protein kinases identifies a conserved activation mechanism, *Proc. Nat. Acad. Sci. USA 103*, 17783-17788.
16. Nagar, B., Hantschel, O., Young, M. A., Scheffzek, K., Veach, D., Bornmann, W., Clarkson, B., Superti-Furga, G., and Kuriyan, J. (2003) Structural Basis for the Autoinhibition of c-Abl Tyrosine Kinase, *Cell 112*, 859-871.
17. Huse, M., and Kuriyan, J. (2002) The Conformational Plasticity of Protein Kinases, *Cell 109*, 275-282.
18. Levinson, N. M., Kuchment, O., Shen, K., Young, M. A., Koldobskiy, M., Karplus, M., Cole, P. A., and Kuriyan, J. (2006) A Src-Like Inactive Conformation in the Abl Tyrosine Kinase Domain, *PLoS Biol. 4*, 0753-0767.
19. Gunasekaran, K., and Nussinov, R. (2007) How Different are Structurally Flexible and Rigid Binding Sites? Sequence and Structural Features Discriminating Proteins that Do and Do not Undergo Conformational Change upon Ligand Binding, *J. Mol. Biol. 365*, 257-273.
20. Shan, Y., Seeliger, M. A., Eastwood, M. P., Frank, F., Xu, H., Jensen, M. O., Dror, R. O., Kuriyan, J., and Shaw, D. E. (2009) A conserved protonation-dependent switch controls drug binding in the Abl kinase, *Proc. Nat. Acad. Sci. USA 106*, 139-144.